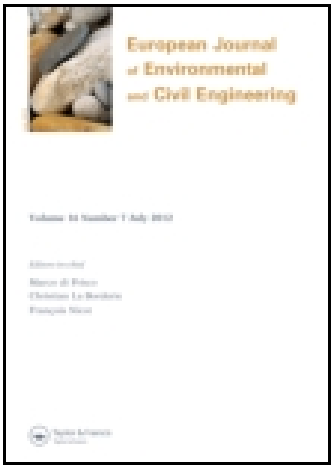

European Journal of Environmental and Civil Engineering

Publication details, including instructions for authors and subscription information:
http://www.tandfonline.com/loi/tece20

Numerical prediction on erosion damage caused by wind-blown sand movement

X.J. Shi[a] & X.F. Shi[b]

[a] Department of Civil Engineering, Tianjin College, University of Science and Technology Beijing, Tianjin 301830, China

[b] School of Mechanical Engineering and Automation, BeiHang University, Beijing 100083, China

Published online: 26 Feb 2014.

To cite this article: X.J. Shi & X.F. Shi (2014) Numerical prediction on erosion damage caused by wind-blown sand movement, European Journal of Environmental and Civil Engineering, 18:5, 550-566, DOI: 10.1080/19648189.2014.891468

To link to this article: http://dx.doi.org/10.1080/19648189.2014.891468

European Journal of Environmental and Civil Engineering, 2014
Vol. 18, No. 5, 550–566, http://dx.doi.org/10.1080/19648189.2014.891468

Numerical prediction on erosion damage caused by wind-blown sand movement

X.J. Shi[a] and X.F. Shi[b]*

[a]*Department of Civil Engineering, Tianjin College, University of Science and Technology Beijing, Tianjin 301830, China;* [b]*School of Mechanical Engineering and Automation, BeiHang University, Beijing 100083, China*

(*Received 15 April 2013; accepted 27 January 2014*)

This study quantitatively investigated the erosion damage on the metal material caused by wind-blown sand under different environmental conditions (e.g. height and wind velocity) in aeolian processes. Wind-blown sand causes destructive impacts on buildings, abrasion of crops and many other damages in arid regions. Sand transport caused by wind often appears in the desert, open-pit mines and coastal dune fields, which is a special case of two-phase flow of gas and solids. Due to its special dynamic characteristics, the sand–wind system near the bed surface is complex and difficult to be solved by traditional computational fluid dynamics method. However, the steady-state saltation model is effective for describing the wind-blown sand movement. Therefore, this paper combines the solid particles erosion model with the steady-state saltation model to predict the erosion damages caused by blown sand. Correctness of the algorithm has been verified through the comparison of simulated results and experimental data of the sand flow structure. An early conclusion that the kinetic energy is crucial to erosion has been proved in this paper. The results show that the erosion rate varies with different variables, e.g. saltating velocity, saltating height, length, etc. The quantity of erosion shows stratification pattern as well as the mass flux of the sand flow. These results quantitatively show the major features of the erosion caused by wind-blown sand.

Keywords: erosion; solid particle erosion; impact; wear modelling

1. Introduction

Solid particle erosion (SPE) is widely found in various engineering, such as the pipelines, valves, water turbines and aerospace equipment, etc. As a form of the SPE, wind-blown sand causes destructive impacts on buildings, abrasion of crops and many other damages in arid regions (Liu, Gao, Shi, Li, & Dong, 2003). In these conditions, sand particles on the surface of the bed obtain energy from the wind. As wind speed increases, sand particles of ~70–500 μm diameter are the first to be moved by wind. After lifting, these particles bounce along the bed surface in a series of hops (Greeley & Iversen, 1985; Shao & Lu, 2000), in a process known as saltation (Figure 1) (Kok & Renno, 2009). A wind-blown sand particle with high saltating and spinning speed possesses potent abrasive capacity (Zou, Liu, & Dong, 1994). It causes severe erosions on the equipment, structures and accelerates their failure.

*Corresponding author. Email: xfshi@me.buaa.edu.cn

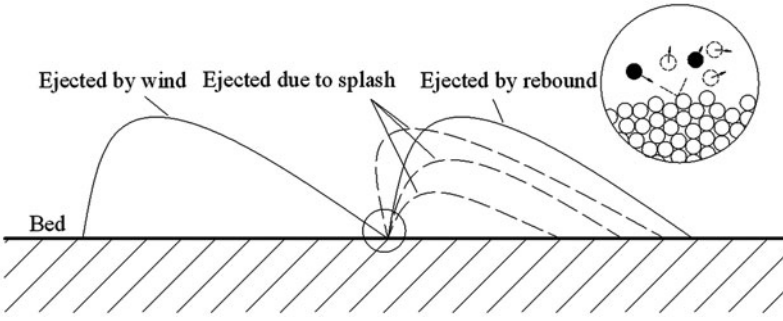

Figure 1. An idealised spherical sand particle propelled by wind changed other particles' motion when it splashed on the bed surface.

In order to quantitatively predict the erosion damage, a few theoretical models containing variables such as particle mass, impact velocity, impact angle and physical properties of the materials have been proposed (Meng & Ludema, 1995). The combination of the models and computational fluid dynamics (CFD) method is a popular way to predict SPE in many important areas of the oil and gas industry. It is practical to estimate the erosion damages resulting from particle impacts (Zhang, Reuterfors, McLaury, Shirazi, & Rybicki, 2007). Researches on these damage predictions are always focused on the area of engineering environment, particularly in certain working conditions (Mbabazi & Sheer, 2006). However, the research on SPE caused by wind-blown sand is seldom seen (Hao, Xing & Yang, 2010; Liu et al., 2003).

Sand transported by wind is a special case of two-phase flow of gas and solids (Anderson & Haff, 1991; Butterfield, 1991) and a transport, sorting and deposition process (White & Mounla, 1991). After the saltation reaches steady state, the amount of sand particles in the air reaches to a saturated state. As there are a large number of sand particles in the air, the retardation of the wind caused by saltating particles cannot be ignored. Zheng, He, and Zhou (2004) propose that the sand particles with charged characteristics are influenced by a greater electrostatic force. Thus, a coupled wind-sand-electricity field's calculation approach needs to be used in solving the wind-sand flow. It is different from the techniques which are often used in the CFD; some difficulties do exist in this approach, including the implementation of the distribution functions of sand particles' lift-off velocities, the evolution of particles' saltating trajectories and the multi-field coupling problems, etc. Mathematical models for simulation of the sand saltation (Anderson & Haff, 1988; Kok & Renno, 2009; Zheng, He, & Wu, 2004) and the erosion prediction (Meng & Ludema, 1995) have been separately developed by researchers. Accordingly, a steady-state saltation model of Zheng et al. (2004) coupled with the Oka, Okamura, and Yoshida' (2005) erosion model is implemented in this paper to quantitatively investigate the erosion damage by sand particles in different environmental conditions (e.g. height, wind velocity, etc.).

2. Theoretical model of saltation-erosion

For prediction of the erosion damage caused by sand particles at arbitrary height z, a control volume (i.e. the quadrature cell) $dxdydz$ at z which contains a number of sand particles with all kinds of velocity of $\boldsymbol{v}$ will be considered (Figure 2). The plane to be

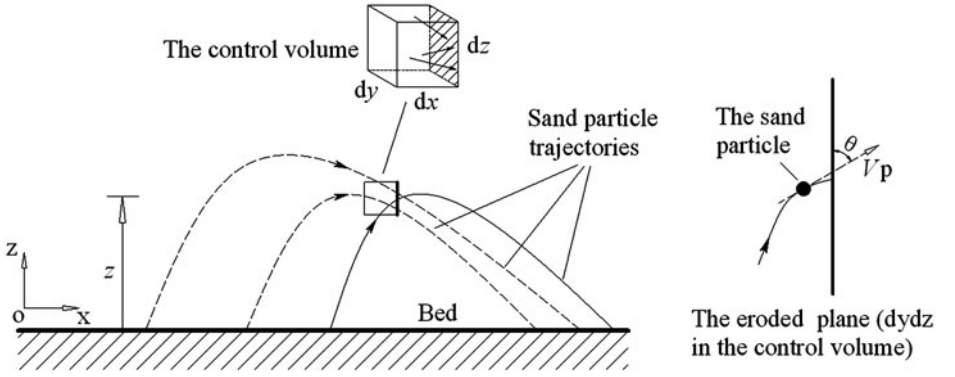

Figure 2. The sketch of erosion damages caused by sand particles during the its ascending and descending process.

eroded is defined as the d*y*d*z* in the control volume, which is impacted by sand particles numbered in the control volume per unit time. The d*y*d*z* is chosen because it is more practical to predict the erosion damage of vertical planes, as many upright panels of facilities and constructions are exposed in the wind–sand flow in the field. Any particle with a velocity of $\boldsymbol{V}_{\mathrm{p}}$ will form an impact angle θ with d*y*d*z* when erosion occurs, see the enlarged view in Figure 2. We obtain the profiles of sand flux/erosion related quantities through the integral of control volumes along the height (i.e. z) direction and thus the integrands are calculated firstly in the control volume. The integrands include numbers of sand particles, the reacting force to the wind by sand particles, the mass flux, the kinetic energy flux of sand and the quantity of erosion (Qe). Accordingly, erosion damage related to quantities at arbitrary height z can be obtained. Specific process is as follows: All kinds of forces acting on one particle including the force of retarding the wind speed are calculated first. Then the kinematics equation for single particle is established. After that, we calculate macroscopic variables of wind–sand flow structure and erosion damage, including the wind speed retardation induced by gross sand particles. Then we adjust the number of sand particles to change the restraining force on wind until the system reaches a steady state and thus steady quantities of the mixed flow and erosion are obtained. Properties of material, impact velocity and size are critical variables for impact-angle dependence of erosion. While the angle θ changes continuously in the process of particle saltation. Therefore, erosion damages vary with the location of the particle in the air and thus the height if x is given (See Figure 2). Besides, there are other factors for its variation, e.g. different sand particle sizes and initial ejecting velocities. Any metal whose relative parameters of properties have been known can be used as the target material. Here we choose Inconel 718 representatively.

2.1. *Coordinate system for the saltating particle*

Considering sand saltating on the infinite and flat sand-bed in the two-dimensional wind field at a steady state, the coordinate system O*xz* shown in Figure 3 is established, in which Axis-x is along the direction of wind field, Axis-z is perpendicular to the Axis-x, u (z) is the logarithmic wind profile, $\boldsymbol{F}_{\mathrm{g}}$ is the gravity of sand particle, $\boldsymbol{F}_{\mathrm{e}}$ is the electrostatic force, $\boldsymbol{F}_{\mathrm{l}}$ is the Saffman force, $\boldsymbol{F}_{\mathrm{d}}$ is the aerodynamic drag force, $\boldsymbol{F}_{\mathrm{m}}$ is the Magnus force.

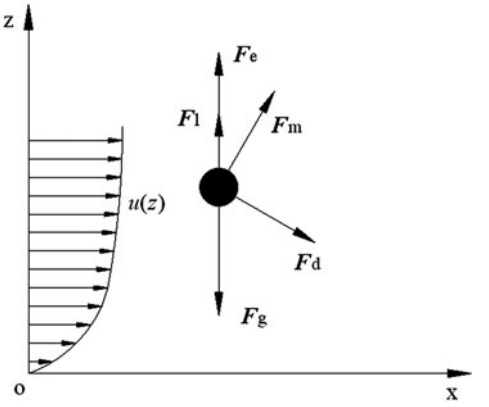

Figure 3. Coordinate system for the saltating particle and forces acting on it.

The forces acting on a spherical sand particle (Anderson & Hallet, 1986; Schmidt, Schmidt, & Dent, 1998) with identical diameter D and uniform density ρ_g in saltation are generally divided into two different groups: forces that have no relation with the relative motion between the wind field and the sand particles: $\boldsymbol{F}_g$, $\boldsymbol{F}_e$ and $\boldsymbol{F}_l$, and those depending on it: $\boldsymbol{F}_d$ and $\boldsymbol{F}_m$. On the basis of Newton's equation and Euler's equation, the fundamental dynamic equations for a single saltating particle can be described by Zheng et al. (2004)

$$\frac{1}{6}\pi\rho_g D^3 \cdot a = \boldsymbol{F}_g + \boldsymbol{F}_e + \boldsymbol{F}_l + \boldsymbol{F}_d + \boldsymbol{F}_m \tag{1}$$

$$\boldsymbol{M} = I \cdot \boldsymbol{\alpha}, \tag{2}$$

where $\boldsymbol{M}$ is the moment of the particle, I is the is the particle's moment of inertia, $\boldsymbol{\alpha}$ is the angular acceleration of the particle. Expressions for forces and related symbols see Appendices 1 and 3.

2.2. *Motion equations of saltating particles*

The mean wind velocity profile u (z) for a steady wind-blown sand flux is described by Navier-Stokes equation (Ungar & Haff, 1987)

$$F_x(z) + \frac{\mathrm{d}}{\mathrm{d}z}\left(\rho_a k^2 \left[z\frac{\mathrm{d}u}{\mathrm{d}z}\right]^2\right) = 0, \tag{3}$$

or

$$\frac{\mathrm{d}^2 u}{\mathrm{d}z^2} = -\frac{1}{z}\frac{\mathrm{d}u}{\mathrm{d}z} - \frac{1}{2\rho_a k^2 z^2 \frac{\mathrm{d}u}{\mathrm{d}z}} F_x(z), \tag{4}$$

where k is Von Karman constant, F_x (z) is the spatially averaged drag force per unit volume of the saltating sand particles on the wind in the horizontal x direction.

The velocity of sand particle ejecting from the bed is a random variable and obeys the distribution function of vertical lift-off velocity f (v_0) (Anderson & Hallet, 1986).

$$f(v_0) = \frac{13.5}{0.96u_*}\left(\frac{v_0}{0.96u_*}\right)^3 \exp\left(-\frac{3v_0}{0.96u_*}\right), \tag{5}$$

where v_0 is the vertical lift-off velocity of ejected particles, and u_* is the friction velocity. The number density of saltating particles N_1 (z) is given by (Anderson & Hallet, 1986).

$$N_1(z) = s\int_0^\infty f(v_0) \times \left(\frac{1}{\dot{z}_\uparrow(v_0,z)} - \frac{1}{\dot{z}_\downarrow(v_0,z)}\right)\mathrm{d}v_0, \tag{6}$$

where s is the surface ejection rate (the number of particles ejected per unit area of the sand bed per unit time). The arrows depict, respectively, upward and downward limbs of trajectory, for each particle in flight will traverse the same height z twice. One dot above the variable means the first-order and two means the second-order time derivative of the corresponding variable.

By Newton's third law, the reaction force per unit volume of the saltating particles on the wind is (Zheng et al., 2004)

$$F_x(z) = -\frac{1}{6}\pi\rho_g s D^3 \int_0^\infty f(v_0) \times \left[\frac{\ddot{x}_\uparrow(v_0,z)}{\dot{z}_\uparrow(v_0,z)} - \frac{\ddot{x}_\downarrow(v_0,z)}{\dot{z}_\downarrow(v_0,z)}\right]\mathrm{d}v_0. \tag{7}$$

On the basis of Equation (6), the vertical profile of mass flux $Q(z)$ and kinetic energy flux $M(z)$ is given by Equations (8) and (9) respectively.

$$Q(z) = \frac{1}{6}\pi\rho_g s D^3 \int_0^\infty f(v_0) \times \left[\frac{\dot{x}_\uparrow(v_0,z)}{\dot{z}_\uparrow(v_0,z)} - \frac{\dot{x}_\downarrow(v_0,z)}{\dot{z}_\downarrow(v_0,z)}\right]\mathrm{d}v_0; \tag{8}$$

$$M(z) = \frac{1}{12}\pi\rho_g s D^3 \int_0^\infty f(v_0) \times \left[\frac{\ddot{x}_\uparrow(v_0,z)}{\dot{z}_\uparrow(v_0,z)} - \frac{\ddot{x}_\downarrow(v_0,z)}{\dot{z}_\downarrow(v_0,z)}\right]\mathrm{d}v_0; \tag{9}$$

Substituting the expressions of forces $\boldsymbol{F}_g$, $\boldsymbol{F}_e$, $\boldsymbol{F}_l$, $\boldsymbol{F}_d$ and $\boldsymbol{F}_m$ summarised in Appendix 1 into Equation (1), the following set of equations is solved to keep track of individual particles.

$$\ddot{x} = 0.75\frac{\rho_a}{\rho_g}\left[\left(\omega - \frac{1}{2}\frac{\partial u}{\partial z}\right)\dot{z} - \frac{C_d}{D}\cdot\sqrt{(\dot{x}-u)^2 + (\dot{z})^2}(\dot{x}-u)\right], \tag{10}$$

$$\begin{aligned}\ddot{z} = 0.75\frac{\rho_a}{\rho_g}&\left[\begin{array}{c} -\left(\omega - \frac{1}{2}\frac{\partial u}{\partial z}\right)(\dot{x}-u) - \frac{C_d}{D}\cdot\sqrt{(\dot{x}-u)^2 + (\dot{z})^2}\dot{z} \\ +0.85\frac{C_d}{D}\left(u_{\mathrm{top}}^2 - u_{\mathrm{bot}}^2\right)\end{array}\right] \\ &- g + 51,000.0(100.0z)^{-0.6}q,\end{aligned} \tag{11}$$

$$\dot{\omega} = \frac{60\mu}{\rho_g D^2}\left(\omega - \frac{1}{2}\frac{\mathrm{d}u}{\mathrm{d}z}\right), \tag{12}$$

The corresponding initial and boundary conditions are:

$$t = 0{:}x = 0, z = 0, \dot{x} = 0, \dot{z} = v_0, \omega = \omega_0; \tag{13}$$

$$z = z_0 : u = 0; \tag{14}$$

$$z \to \infty : zk\frac{\mathrm{d}u}{\mathrm{d}z} = u_*; \tag{15}$$

where z_0 is the aerodynamic roughness, given as $z_0 = D/30$ (Ungar & Haff, 1987). Thus the above equations constitute the theoretical model for the sand saltation in the coupled wind-sand-electricity fields.

2.3. Calculation of erosion damage during saltation process

Since we have details of the steady-state saltation such as velocity, trajectory of particles, etc., the erosion damage caused by moving sand particles can be evaluated. The erosion model of Oka & Yoshida (2005) is presented below:

$$E(\theta) = g(\theta)E_{90}; \tag{16}$$

$$g(\theta) = (\sin\theta)^{n1}(1 + Hv(1 - \sin\theta))^{n2}; \tag{17}$$

$$E_{90} = K(Hv)^{k1}\left(\frac{V_p}{V'}\right)^{k2}\left(\frac{D}{D'}\right)^{k3}; \tag{18}$$

$$n1 = s1(Hv)^{q1}; n2 = s2(Hv)^{q2}; k2 = 2.3(Hv)^{0.038}. \tag{19}$$

where $E(\theta)$ is the erosion damage ($mm^3\,kg^{-1}$) at an arbitrary impact angle; E_{90} is the erosion damage ($mm^3\,kg^{-1}$) at normal impact angle; both of $E(\theta)$ and E_{90} denote the volume of target material removed by per unit mass of particles, but for different impact angle; V_p and V' are the particle impact speed and the reference impact speed, respectively; D and D' are the particle diameter and the reference diameter, respectively; Hv is the Vickers' number in GPa, indicating the target material hardness. In these parameters, V_p can be obtained through the saltation model. V' and D' are standard value used in the erosion experiments for the correlations of erosion damage. The $n1$ and $n2$ are experimentally obtained by Oka et al. (2005). It was considered that the constants and exponents of K, $k1$, $k3$, particularly $k2$ take individual values based on the type of particle, since the particle property which includes such as particle shape, angularity and hardness is not correlated with the impact conditions and other factors (Oka & Yoshida, 2005). The use of the parameter is according to the assumption that a sand particle is supposed to an approximate sphere of SiO_2 material. See Appendix 2 for related parameter details. θ is described by the particle impact speed V_p (See Figure 2) and calculated by $\dot{x}, \dot{z}$

$$\sin\theta_{\uparrow(\downarrow)} = \dot{x}_{\uparrow(\downarrow)}(v_0, z)/V_{p\uparrow(\downarrow)}; V_{p\uparrow(\downarrow)} = \sqrt{[\dot{x}_{\uparrow(\downarrow)}(v_0, z)]^2 + [\dot{z}_{\uparrow(\downarrow)}(v_0, z)]^2}. \tag{20}$$

With a given lift-off velocity v_0, $\sin\theta$ is a function of the saltating height z in a steady flow field considering that $\dot{x}$ and $\dot{z}$ both vary with z. Thus the impact angle dependence of erosion $E(\theta)$ (Equation 16) can be transformed to $E(v_0, z)$.

$$\begin{aligned} E_{\uparrow(\downarrow)}(v_0, z) = {} & (\dot{x}_{\uparrow(\downarrow)}(v_0, z)/\sqrt{[\dot{x}_{\uparrow(\downarrow)}(v_0, z)]^2 + [\dot{z}_{\uparrow(\downarrow)}(v_0, z)]^2})^{n1} \\ & \times (1 + Hv(1 - \dot{x}_{\uparrow(\downarrow)}(v_0, z)/\sqrt{[\dot{x}_{\uparrow(\downarrow)}(v_0, z)]^2 + [\dot{z}_{\uparrow(\downarrow)}(v_0, z)]^2}))^{n2} \\ & \times K(Hv)^{k1}\left(\frac{\sqrt{[\dot{x}_{\uparrow(\downarrow)}(v_0, z)]^2 + [\dot{z}_{\uparrow(\downarrow)}(v_0, z)]^2}}{V'}\right)^{k2}\left(\frac{D}{D'}\right)^{k3}, \end{aligned} \tag{21}$$

Therefore, the specific Qe (Equation 22) at a given height z can be calculated according to the definition of E (Equation 21) and the number density of hopping particles (Equation 6).

$$Qe(z) = \frac{1}{6}\pi\rho_g s D^3 \int_0^\infty f(v_0) \times \left[\frac{E_\uparrow(v_0,z)}{\dot{z}_\uparrow(v_0,z)} - \frac{E_\downarrow(v_0,z)}{\dot{z}_\downarrow(v_0,z)}\right] \mathrm{d}v_0, \tag{22}$$

With Equations (6) and (22), the average erosion rate E_{avg} of the control volume at z is given by

$$E_{\mathrm{avg}}(z) = \frac{Qe(z)}{N(z) \times \frac{1}{6}\rho_g \pi D^3}, \tag{23}$$

$$|Q_*|(z) = \frac{1}{6}\pi\rho_g s D^3 \int_0^\infty f(v_0) \times \left[\frac{|V_p|_\uparrow}{\dot{z}_\uparrow(v_0,z)} - \frac{|V_p|_\downarrow}{\dot{z}_\downarrow(v_0,z)}\right] \mathrm{d}v_0. \tag{24}$$

$$|V_p|_{\mathrm{avg}}(z) = \frac{|Q_*|(z)}{N(z) \times \frac{1}{6}\rho_g \pi D^3}. \tag{25}$$

where $E_{\mathrm{avg}}(z)$ means that the total value of $E_\uparrow(v_0, z)$ and $E_\downarrow(v_0, z)$ with all kinds of v_0 (see Equation (5)) in the control volume at z is averaged. We define it here to find how erosion rate varies with height eliminating the influence of the number density of the sand particles. The average resultant velocity $|V_p|_{\mathrm{avg}}(z)$ of particles can be calculated with Equations (6) and (24). The average resultant velocity $|V_p|_{\mathrm{avg}}(z)$ is a quantity which describes the features of particles' various resultant velocities at height z. Where $|Q_*|(z)$ is a preparation for the calculation of $|V_p|_{\mathrm{avg}}(z)$. $|Q_*|(z)$ is the integral of the total momentum of particles with different velocities in the control volume at z. note that: $|Q_*|(z)$ is different from $Q(z)$ as the latter is the integral of the horizontal component of the particles' momentum.

3. Algorithm for calculation

A complementary condition is needed to determine s in Equations (6)–(9), Equations (22) and (24), which makes the wind-blown sand movement maintained at the steady state.

Owen (1964) pointed out that the shear-stress exerted by the wind on the sand bed surface should be equal to that of the impact threshold wind given by Bagnold (1941) when the wind-blown sand flux achieves its balance, that is,

$$z = z_0 : \frac{du}{dz} = \frac{0.08}{kz_0}\sqrt{\frac{\rho_g - \rho_a}{\rho_a} gD}. \tag{26}$$

where ρ_a is the air density; ρ_g is sand particle density; g is the gravity acceleration; D is the particle diameter; k is Von Karman constant; z_0 is the aerodynamic roughness, given as $z_0 = D/30$ (Ungar & Haff, 1987). The value of these parameters can be seen in Appendix 3. Thus replacing the boundary condition of Equation (15) by the initial condition of Equation (26), the basic equations of the saltation model in the coupled wind-sand-electric fields can be solved by Runge-Kutta procedure. The non-linear parts of the model are treated by using the iterative method. Finally, the boundary condition of Equation (15) could be satisfied by adjusting the surface ejection rate s. In the whole process, parameters as k, g and ρ, etc. (see Appendix 3) are treated as constants. The

detailed computing procedure is described as follows. The initial s, du/dz, $u(z)$ and u_* is regarded as input to calculate the time derivatives of x and z. We then obtain the $F_x(z)$ through the time derivatives of x and z. After that, the wind velocity $u(z)$ sustaining $F_x(z)$ is calculated. The first convergent criterion is that $u(z)$ reaches its steady state, that is, $u^{(i)}(z) - u^{(i-1)}(z) < \varepsilon_1$, where i is the iterative step, ε is an arbitrary small number. After $u(z)$ reaching its steady state, the convergence of $u_*(z)$ will be judged. If $u_*{}^{(i)}(z) - u_* < \varepsilon_2$, the program will output the value of $N(z)$, $Q(z)$, $M(z)$, $Qe(z)$ etc. The detailed flow chart is described in Figure 4.

4. Validity of the numerical model

Validation of the numerical program based on the steady-state saltation model has been made. That is, comparisons of the relation between the sand transport rate Q_0 and friction velocity u_* with those obtained using the well-known empirical formulas of transport rate given by Bagnold (1941) and Kawamura (1951) will be made. The sand transport rate Q_0 is defined as the mass of sand carried by wind per unit of time and per unit of the width. Q_0 is derived by vertical direction integral of $Q(z)$ based on Equation (8).

$$Q_0 = \int_0^\infty Q(z)\mathrm{d}z. \tag{27}$$

The Bagnold (1941) formula and the Kawamura (1951) formula are expressed as:

$$Q_0 = C\frac{\rho_a}{g}\sqrt{\frac{D}{0.00025}}u_*^3, \tag{28}$$

$$Q_0 = K\frac{\rho_a}{g}(u_* - u_{*t})(u_* + u_{*t})^2, \tag{29}$$

where the $C = 1.5$ and $K = 1.0$ for nearly uniform sand particles. According to experimental research, the Kawamura's formula is suitable for the condition of $u_* < 0.4$ ms^{-1}; while for $0.4\,\mathrm{ms}^{-1} < u_* < 0.7\,\mathrm{ms}^{-1}$, Bagnold's formula is more effective. With the increment of u_*, both values of formulas are smaller than the experimental data. Results of both formulas and the model introduced by this paper are plotted in Figure 5, where particles diameter $D = 0.25$ mm. It can be found in Figure 5 that, for $u_* < 0.5\,\mathrm{ms}^{-1}$, the numerical results are very close to the value given by formula (29); while for $u_* > 0.6\,\mathrm{ms}^{-1}$, the results are close to the value given by formula (28). Compared all the results in Figure 5, it is obvious that the sand transport rates calculated in this paper agree well with those obtained from Bagnold's and Kawamura's empirical formulas in their respective effective regions, demonstrating that the model and the algorithm used in this paper are correct and effective in the problems of wind-blown sand movement.

5. Results and discussion

5.1. *Qe caused by wind-sand flow*

The mass flux is one of the most important quantities of macro-variables for wind-sand structure. We found that the erosion damage (in the following it will be called Qe, to be precise) has the similar profile with the mass flux of sand. We further compared the profile of the kinetic energy flux of sand with Qe to make a better understanding of wind–sand

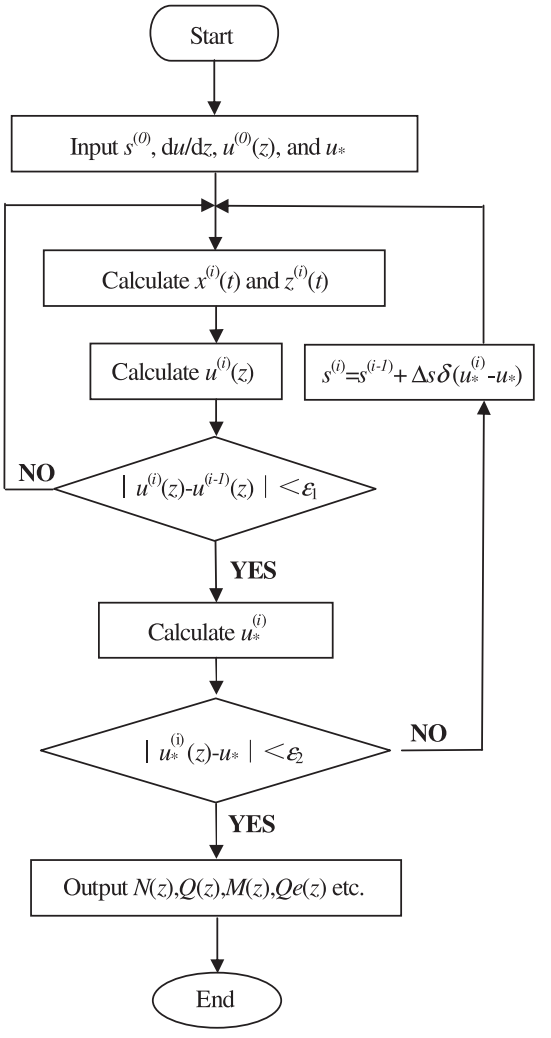

Figure 4. The flow chart for the calculation of the saltation model in the coupled wind-sand-electricity fields.

caused erosion. Stratification pattern of the Qe profile has been found in Figures 6 and 7. Three layers exist in the Qe profile at steady state, which are monotonic increment layer, the saturation layer and the monotonic decrement layer, respectively. There is also a peak value of height called the saturation height correspondingly. The similar stratification pattern of vertical mass flux profile and kinetic energy flux profile at steady state has been researched by Zheng et al. (2004). All of these three profiles increase first and then decrease with the increment of height. This can be verified by the experiment of Liu et al. (2003), in which they made wind tunnel measurement of adobe erosion (which is called abrasion their article). They also obtained an abrasion rate maximum at a certain height above the ground and called it $H_{\max}$. In this numerical test, the uniform diameters of sand particles are 0.3 mm and the charge-to-mass ratio q are 60 μC kg^{-1}. The friction velocity is 0.69 ms^{-1}. The most severe erosion (1.75×10^{-4} mm^3 m^{-2}s^{-1}) occurs at the height of ca.

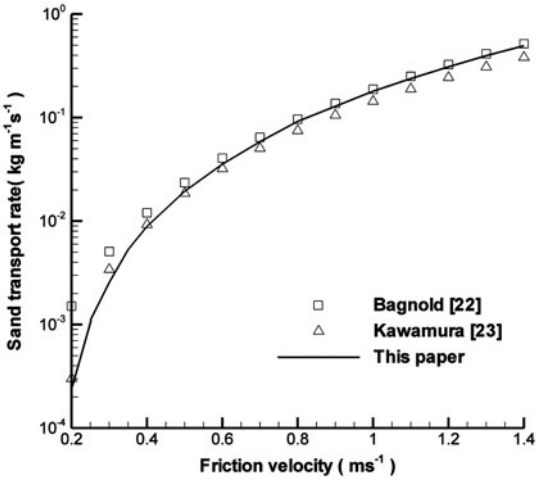

Figure 5. Comparison of the relationships between the sand transport rate and the friction velocity calculated in this paper with the empirical formulas given by Bagnold and Kawamura.

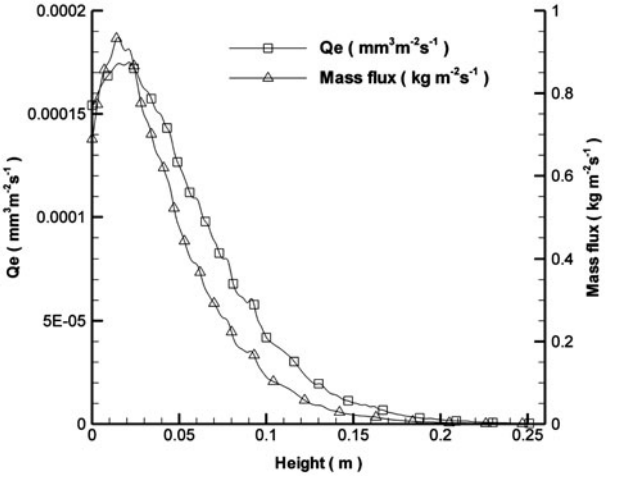

Figure 6. The variations of the *Qe* and the profile of Mass flux with Height at steady state ($D = 0.3$ mm, $u_* = 0.69\ \mathrm{ms}^{-1}$, $q = 60\ \mu\mathrm{C\ kg}^{-1}$).

0.025 m, where the kinetic energy flux also reaches its maximum of $1.9\ \mathrm{J\ m}^{-2}\ \mathrm{s}^{-1}$, while the peak of $0.95\ \mathrm{kg\ m}^{-2}\ \mathrm{s}^{-1}$ occurs at another height of ca. 0.015 m for mass flux. Thus the profile shape of *Qe* has a better match with that of kinetic energy flux, which is in accordance with the conclusion that "Correlative equations with erosion damage are generally derived from particle impact energy" (Oka & Yoshida, 2005).

The wind velocity is crucial to *Qe*, as the wind is the continuous energy supply to erosion. Given that the uniform diameter of sand particles $D = 0.3$ mm and the charge-to-mass ratio $q = 60\ \mu\mathrm{C\ kg}^{-1}$, the distributions of the *Qe* with height under different friction velocities (0.34, 0.51, $0.69\ \mathrm{ms}^{-1}$ respectively) are shown in Figure 8. It can be found that

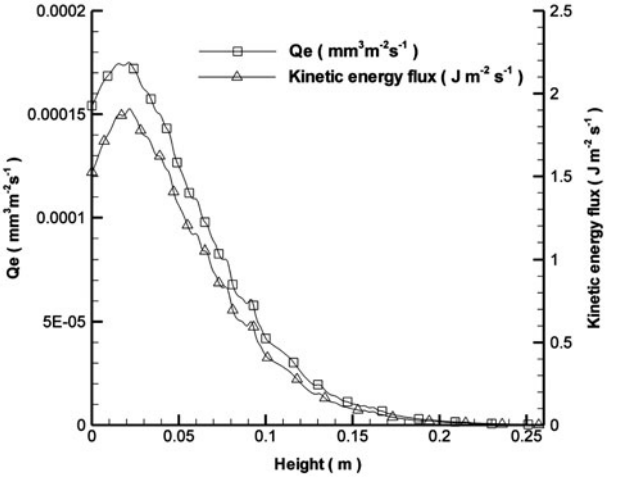

Figure 7. The variations of the *Qe* and the profile of kinetic energy flux with Height at steady state. ($D = 0.3$ mm, $u_* = 0.69\ \mathrm{ms}^{-1}$, $q = 60\ \mu\mathrm{C\ kg}^{-1}$).

all the three profiles have the similar pattern. Liu et al. (2003) also concluded that the patterns of the abrasion profiles were similar to one another and observed that the $H_{\max}$ shifted upward when wind velocity increased in their experiments. In our simulation, the maximum of *Qe* of $8.3 \times 10^{-5}\ \mathrm{mm^3\ m^{-2}s^{-1}}$ is at the height of 0.0085 m when u_* is $0.51\ \mathrm{ms}^{-1}$, while the peak of *Qe* is $2.1 \times 10^{-4}\ \mathrm{mm^3\ m^{-2}s^{-1}}$ for u_* of $0.69\ \mathrm{ms}^{-1}$ with the corresponding height raised at 0.022 m. With the increment of the wind velocity, *Qe* increases greatly and the peak height of *Qe* is also raised. However, the peak is not distinct in the *Qe* profile when the shear velocity is small, such as $0.34\ \mathrm{ms}^{-1}$ in this figure. The number of particles with the small lift-off velocity is dominating as the effect of the lower shear velocity and thus most of the particles saltate very near the bed. This also leads to an indistinct peak value of *Qe* close to the zero height.

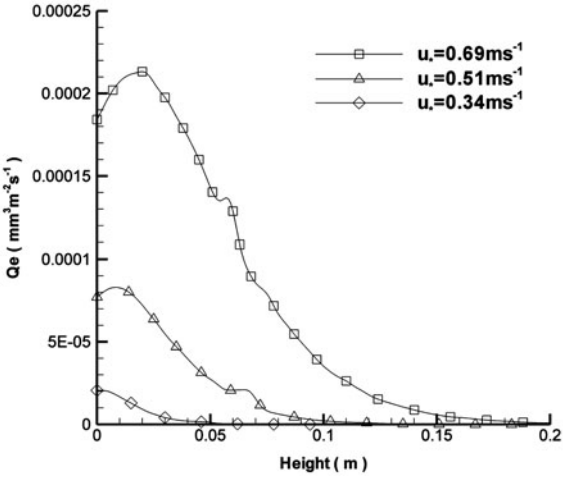

Figure 8. The variations of the *Qe* with Height with different u_* at steady state ($D = 0.3$ mm, $u_* = 0.69\ \mathrm{ms}^{-1}$, $q = 60\ \mu\mathrm{C\ kg}^{-1}$).

5.2. Erosive capacity of sand particle

The erosion rate E is an index of the erosive capacity of sand particles. Note that E varies with particle impact velocity V_p, impact angle θ and particle diameters D for the same target material. Both the V_p and θ are transient during the particle hopping process. The particle trajectory is the function of V_p and θ, through which we discuss the combined effect of V_p and θ on erosion rate. The variation of the erosion rate in solid lines and the saltating height in dash lines with the saltation length (i.e. saltation distance, which is the distance the particle has travelled from lifting off to splashing on the bed) are shown in Figure 9. With the fixed diameter D of 0.25 mm, the hopping trajectories are determined by lift-off velocities v_0 given the charge-to-mass ratio q of 60 μC kg^{-1}and the friction velocity u_* of 0.69 ms^{-1}. Four lift-off velocities (v_0) of 5.0, 4.0, 2.5 and 1.0 ms^{-1} are chosen here and four kinds of trajectories are obtained. We can make comparisons between the erosion rate and the particle trajectory with the common x-axis and thus it may help to reveal the relation between the erosion rate and the positions of sand particles in the air. The E is zero after the sand splashing on the bed, e.g. the E is zero at the length greater than ca. 0.31 m for v_0 of 5.0 ms^{-1}. For particle with a fixed v_0, the E increases first and then declines, with the existence of a peak value. The corresponding location in the trajectory of E can be tracked by the variable of saltating length. For instance, given that $v_0 = 4.0$ ms^{-1}, the vertical displacement of particle reaches its maximum of ca.0.25 m as the saltating length is 0.6 m, while the corresponding E is only 0.0040 mm^3 kg^{-1}. The E reaches its peak of 0.0068 mm^3 kg^{-1} at the length of 2 m, while the vertical displacement of particle has dropped to ca. 0.1 m. The maximum E appears in the downward limb of particle trajectory. The reason of the increase of E with length is that V_p is promoted constantly by wind as the height increasing before the maximum. The decrease after the maximum is because the falling of the relative high speed of particles when entering into the near surface and thus V_p is retarded. As is well known, the logarithmic wind profile leads to a rapid decline of wind speed near the bed surface. We also found that the maximum of E lags behind that of saltation height. The erosion is caused by the combined effects of repeated plastic deformation and cutting action, which determined mainly through the factors of particle velocity

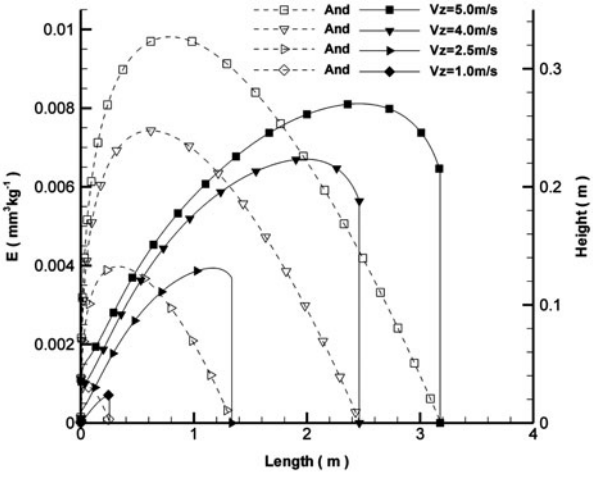

Figure 9. The variations of erosion rate (E) in solid lines and the saltating Height in dash lines with the saltating Length at steady state. ($D = 0.25$ mm, $u_* = 0.69$ ms^{-1}, $q = 60$ μC kg^{-1}).

magnitude and angle in terms of mutual actions. The most severe erosion occurs when the impact angle ranges from 30° to 60° (Oka & Yoshida, 2005). The simultaneous occurrence of the maximum particle velocity and the most erosive impact angle in the downward limb of the trajectory mainly contributes to the peak value of E. This is also the exact reason of the lag between that maximum of E and the peak of the trajectory. Besides, E increases greatly with the increment of lift-off velocity as 1.0, 2.5, 4.0 and 5.0 ms^{-1}, respectively (Figure 9). This also indicates that V_p is crucial to the erosion damages caused by blown sand.

The results of the average erosion rate $E_{avg}(z)$ in solid lines and the average magnitude of particles' velocities $|V_p|_{avg}$ in dash lines in the diameter condition of 0.2, 0.3 and 0.4 mm are shown in Figure 10, respectively. Given the same particles diameter, both $E_{avg}(z)$ and $|V_p|_{avg}$ increases with height within the corresponding range of saltating length. The gradient of $|V_p|_{avg}$ becomes smaller and smaller as the height increases, while the gradient of $E_{avg}(z)$ nearly retains constant. It shows that the higher in the air the larger velocity the sand particle carries. Although the erosion ability of particles at higher height is notable, the Qe is not large because the number density of particles is small. It can be found from Figure 10 that the $E_{avg}(z)$ of the smaller particles (e.g. 0.2 mm) is greater than that of larger particles (e.g. 0.4 mm) within saltation height range (ca. 0–0.26 m). This is because that the $|V_p|_{avg}$ of smaller particles (e.g. 0.2 mm) is also greater than that of larger particles (e.g. 0.4 mm) at the same range (ca. 0–0.26 m). Smaller particles always carry greater velocity and the kinetic energy in the same wind field, which contributes to the greater erosion rate.

5.3. *Some further discussions on the model's effectiveness*

Most of the erosion models including the model used in this paper are developed for particles with high velocities in airflow. The particles possess much greater velocities in

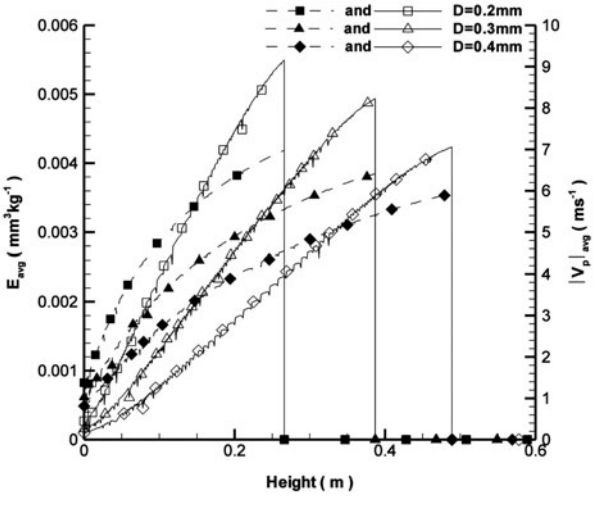

Figure 10. The variations of the average erosion rate E_{avg} in solid lines and the average magnitude of particles' velocities $|V_p|_{avg}$ in dash lines with the Height at steady state. ($u_* = 0.69$ ms^{-1}, $q = 60$ μC kg^{-1}).

Oka et al's experiment than those driven by near bed wind. However, in spite of the fact that the erosion model is developed with relatively greater diameter and at relatively high velocities, it is claimed that the model is applicable "under any impact conditions and for any type of material" (Oka & Yoshida, 2005). Its capability of working with fine particles at low velocity also has been proved (Zhang et al., 2007).

Compared with particles shot from a sand blast type erosion test rig which acquire relative high impact velocities (Oka, Nishimura, Nagahashi, & Matsumura, 2001), the sand particles driven by steady wind has a weak impact ability. Accordingly, the erosion test is quite consuming particularly for metal target materials in the wind-blown circumstances. We have no erosion experimental data to validate directly the numerical results mostly due to this reason. Related experiments have also seldom been seen. In the present research, the comparisons only made qualitatively between parts of the results with that of experiment used of artificial adobe material (Liu et al., 2003). Thus an effective erosion experiment needs to be developed in our next work, which can quantitatively validate the metal erosion model. On the other hand, the numerical simulation is a good way for predicting the erosion damage in the engineering.

The wind-blown sand flux occurs intermittently in the field; it is maintained at the steady state on the premise that the friction velocity of wind is greater than the threshold value. The erosion damage is small for short-term steady-state saltation. But it cannot be ignored for those equipments and building structures long-time exposed in the field. Our model may offer some help for protection of them by predicting the damage before wind erosion and sand storms occurs.

However, this theory established on the condition that saltation happens on the infinite and flat sand-bed; it is not suitable for the environment that the wind field changes sharply. But, the wind direction changes on the premises that it is very close to the object, at that very moment the impact happens or already happened because of particles' inertia. Thus this theory is applicable to simple structures to some extent and with general significance.

6. Conclusions

Based on the steady-state saltation theory and erosion model of Oka and Yoshida (2005), a quantitatively investigation for estimating erosion damage of the equipment with a vertical plane exposing in the wind-blown sand flow has been performed. This investigation analysed the variations of the Qe and erosion rate with height under different conditions, e.g. wind speed, diameter of the sand, etc.

Erosion caused by blown sand always appears near the bed surface, below ca. 0.2 m. The Qe caused by per unit volume of the saltating particles shows distinct stratification pattern. Qe increases with height first and then decreases, a peak value exists. Variations of Qe are more matchable with the kinetic energy flux, showing that the kinetic energy of sand is crucial to erosion. Qe increases fast and the height corresponding to the maximum of Qe become higher, as the wind speed increases.

Erosion rate (E) increases as the lift-off velocity of sand particles (v_0) increases. With a given v_0, E increases first and then decreases; there is also a peak value of E in the downward limbs of particle trajectory. Given the same particles diameter, both of the average erosion rate ($E_{\mathrm{avg}}(z)$) and the average magnitude of particles' velocities ($|V_p|_{\mathrm{avg}}$) increases with height within the corresponding range of saltating length. Smaller particles always carry greater velocity and the kinetic energy in the same wind field, which contributes to the greater erosion rate.

References

Anderson, R. S., & Hallet, B. (1986). Sediment transport by wind: Toward a general model. *GSA Bulletin, 97*, 523–535.

Anderson, R. S., & Haff, P. K. (1988). Simulation of eolian saltation. *Science, 241*, 820–823.

Bagnold, R. A. (1941). *The physics of blown sand and desert dunes*. New York, NY: William Marrow.

Butterfield, G. R. (1991). Grain transport rates in steady and unsteady turbulent airflows. *Acta Mechanica, 1*, 97–122.

Greeley, R., & Iversen, J. D. (1985). *Wind as a geological process on Earth, Mars, Venus, and Titan*. New York, NY: Cambridge University Press.

Hao, Y. H., Xing, Y. M., & Yang, S. T. (2010). Erosion-wear behavior of steel structure coating subject to sandstorm. *Tribology, 30*, 26–31. (in Chinese).

Kawamura, R. (1951). Study on sand movement by wind. *Report of Institution of Science and Technology, 5*, 95–112.

Kok, J. F., & Renno, N. O. (2009). A comprehensive numerical model of steady state saltation (COMSALT). *Journal of Geophysical Research, 114*, D17204.

Liu, L. Y., Gao, S. Y., Shi, P. J., Li, X. Y., & Dong, Z. B. (2003). Wind tunnel measurements of adobe abrasion by blown sand: Profile characteristics in relation to wind velocity and sand flux. *Journal of Arid Environments, 53*, 351–363.

Mbabazi, J. G., & Sheer, T. J. (2006). Computational prediction of erosion of air heater elements by fly ash particles. *Wear, 261*, 1322–1336.

Meng, H. C., & Ludema, K. C. (1995). Wear models and predictive equations: Their form and content. *Wear, 181–183*, 443–457.

Morsi, S. A., & Alexander, A. J. (1972). An investigation of particle trajectories in two –phase flow systems. *Journal of Fluid Mechanics, 11*, 447–459.

Oka, Y. I., Nishimura, M., Nagahashi, K., & Matsumura, M. (2001). Control and evaluation of particle impact conditions in a sand erosion test facility. *Wear, 250*, 736–743.

Oka, Y. I., Okamura, K., & Yoshida, T. (2005). Practical estimation of erosion damage caused by solid particle impact. Part 1: Effects of impact parameters on a predictive equation. *Wear, 259*, 95–101.

Oka, Y. I., & Yoshida, T. (2005). Practical estimation of erosion damage caused by solid particle impact. Part 2: Mechanical properties of materials directly associated with erosion damage. *Wear, 259*, 102–109.

Owen, P. R. (1964). Saltation of uniform grains in air. *Journal of Fluid Mechanics, 20*, 225–242.

Schmidt, D. S., Schmidt, R. A., & Dent, J. D. (1998). Electrostatic force on saltating sand. *Journal of Geophysical Research, 103*, 8997–9001.

Shao, Y. P., & Lu, H. (2000). A simple expression for wind erosion threshold friction velocity. *Journal of Geophysical Research, 105*, 22437–22443.

Ungar, J. E., & Haff, P. K. (1987). Steady state saltation in air. *Sedimentology, 34*, 289–299.

White, B. R., & Schulz, J. C. (1977). Magnus effect in saltation. *Journal of Fluid Mechanics, 81*, 497–512.

White, F. (1974). *Viscous fluid flow*. New York, NY: McGraw-Hill.

Zhang, Y., Reuterfors, E. P., McLaury, B. S., Shirazi, S. A., & Rybicki, E. F. (2007). Comparison of computed and measured particle velocities and erosion in water and air flows. *Wear, 263*, 330–338.

Zheng, X. J., He, L. H., & Wu, J. J. (2004). Vertical profiles of mass flux for windblown sand movement at steady state. *Journal of Geophysical Research, 109*, B01106.

Zheng, X. J., He, L. H., & Zhou, Y. H. (2004). Theoretical model of the electric field produced by charged particles in windblown sand flux. *Journal of Geophysical Research, 109*, D15208.

Zou, X. Y., Liu, Y. Z., & Dong, G. R. (1994). Tentative calculation of wind-sand current energy. *Chinese Science Bulletin, 39*, 1016–1020.

Appendix 1. Expressions of forces acting on a particle and its related symbols

The electrostatic force is taken as

$$\boldsymbol{F}_{\mathrm{e}} = \frac{1}{6}\pi\rho_{\mathrm{g}}D^3 q\boldsymbol{E}, \tag{A.1}$$

in which q is the average charge-to-mass ratio on saltating particles, $\boldsymbol{E}$ is the electric field, the total electric field due to the charged sand particles may be written as (Schmidt et al., 1998)

$$E_z = 51,000.0(100.0z)^{-0.6}. \tag{A.2}$$

The magnitude of lift force $\boldsymbol{F}_{\mathrm{l}}$ is expressed as (Anderson & Hallet, 1986)

$$F_l = \frac{1}{8}\pi D^2\rho_{\mathrm{a}}C_l(u_{\mathrm{top}}^2 - u_{\mathrm{bot}}^2), \tag{A.3}$$

in which u_{top} and u_{bot} are the wind velocities at the heights corresponding to the top and bottom of the particle, respectively. The lift coefficient C_{l} is taken to be $0.85C_{\mathrm{d}}$ (Anderson & Hallet, 1986). The aerodynamic drag force $\boldsymbol{F}_{\mathrm{d}}$ on the particle is expressed as

$$\boldsymbol{F}_d = \frac{1}{8}\pi D^2\rho_{\mathrm{a}}C_{\mathrm{d}}V_r\boldsymbol{V}_r, \tag{A.4}$$

in which $\boldsymbol{V}_r = [(\dot{x}-u)^2 + (\dot{z})^2]^{1/2}$ is the velocity of particle relative to the wind, C_d is the drag coefficient which is the most important parameters to determine the particle trajectory. The drag coefficient of a sphere is strongly dependent on the Reynolds number. A number of empirical representations for this dependence have been developed. The best of these is given in the paper by Morsi and Alexander (1972), who derived a set of equations expressing the relationships between the drag coefficient and Reynolds number over entire Reynolds number range. The equation used in the present research is the best for slatation problems (White, 1974; White & Schulz, 1977),

$$C_d = \frac{24.0}{\mathrm{Re}} + \frac{6.0}{(1.0+\sqrt{\mathrm{Re}})} + 0.4, \tag{A.5}$$

where the Reynolds number Re is defined by $Re = V_{\mathrm{r}}D/v$ and v is the kinetic viscosity of air. The Magnus lift force on a rotating particle is (White & Schulz, 1977)

$$\boldsymbol{F}_m = \pi\rho_{\mathrm{a}}\frac{D^3}{8}\left(\omega - \frac{1}{2}\frac{\partial \boldsymbol{u}}{\partial z}\right). \tag{A.6}$$

Through the angular velocity ω, it is coupled to the moment of the particle

$$\boldsymbol{M} = \pi\mu D^3\left(\omega - \frac{1}{2}\frac{\partial \boldsymbol{u}}{\partial z}\right), \tag{A.7}$$

where μ denotes the dynamic viscosity of the air. I is the particle's moment of inertia given by

$$I = \frac{1}{60}\pi\rho_{\mathrm{g}}D^5. \tag{A.8}$$

Appendix 2. Parameters for the erosion model of Oka & Yoshida (2005)

Parameter	$s1$	$s2$	$q1$	$q2$	K
Value	0.71	2.4	0.14	−0.94	65
Parameter	$k1$	$k3$	V'	D'	
Value	−0.12	0.19	104 ms^{-1}	326 μm	

Appendix 3. Parameters for the theoretical model of saltation

Parameter	Definition	Value
k	Von Karman's constant	0.4
g	The acceleration of gravity	9.8 ms^{-2}
ρ_a	Air density	1.23 $kg\,m^{-3}$
v	Kinematic viscosity of air	$1.46 \times 10^{-5} m^2\,s^{-1}$
μ	Dynamic viscosity of air	$1.76 \times 10^{-5} kg\,m^{-1}s^{-1}$
ρ_g	Particle density	2650.0 $kg\,m^{-3}$
ω_0	Initial angular velocity	80 rev s^{-1}